

Quantum interference in intentionally disordered doped GaAs/Al_xGa_{1-x}As superlattices

A. J. Chiquito,¹ Yu. A. Pusep,¹ G. M. Gusev,² and A. I. Toropov³

¹*Instituto de Física de São Carlos, Universidade de São Paulo, 13560-970 São Carlos, SP, Brazil*

²*Instituto de Física da Universidade, São Paulo, 05315-970 São Paulo, SP, Brazil*

³*Institute of Semiconductor Physics, 630090 Novosibirsk, Russia*

(Received 28 January 2002; revised manuscript received 11 April 2002; published 22 July 2002)

The processes of quantum interference are studied in intentionally disordered doped short-period GaAs/Al_xGa_{1-x}As superlattices where the conductivity can be controlled by the artificial disorder. We found that the usual formula for the weak localization correction to the classical conductivity of superlattices obtained in the propagative Fermi-surface approximation [W. Szott, C. Jedrzejek, and W.P. Kirk, Phys. Rev. Lett. **63**, 1980 (1989)] does not allow to one explain the observed negative magnetoresistance. An excellent agreement was obtained between our results and recently published calculations of the quantum interference correction to the conductivity of the strongly disordered superlattices, where the transport regime corresponding to the diffusive Fermi surface was considered [A. Cassam-Chenai and D. Mailly, Phys. Rev. B **52**, 1984 (1995)]. We found a tendency toward a propagative regime with an increase of the electron concentration, when the influence of disorder was weakened. The decrease of the dephasing of the electron wave function was observed with an increase of both the doping concentration and the disorder strength. The observed temperature dependence of the dephasing time manifested that the process of the dephasing is modified in the presence of strong disorder.

DOI: 10.1103/PhysRevB.66.035323

PACS number(s): 71.55.Eq, 71.55.Jv, 72.20.Fr

I. INTRODUCTION

Quantum interference corrections to conductivity cause a negative magnetoresistance of weakly disordered semiconductors.^{1,2} In such materials transport is accompanied by the quantum interference between the electron wave functions, which is known as a weak localization of electrons. Weak-localization corrections determine the magnetoresistance in weak magnetic fields $\omega_c \tau \ll 1$, when the electron-electron interaction can be neglected.³ Disorder plays a considerable role in the weak localization, providing two coherent scattering processes that contribute to the quantum interference. Early perturbative theories of weak localization were developed in the limit of weak disorder,⁴ when the mean free path of electron (λ) is much larger than the Fermi wavelength, i.e., $k_F \lambda \gg 1$, where k_F is the Fermi momentum. As mentioned in Refs. 5 and 6, in the case of strong disorder the quantum corrections to the conductivity become even more relevant. At high disorder, when $k_F \lambda \lesssim 1$, different approaches were used to account for the quantum interference. In the first publication⁷ the interference effects were considered among various paths associated with hopping between localized sites; then a negative magnetoresistance linear in the magnetic field was obtained. A theory of the magnetoresistance in the variable-range-hopping regime employing the critical percolation path picture yielded the quadratic field dependence.⁸ More recent calculations, based on a self-consistent approach of Anderson localization, revealed a similar quadratic dependence for small magnetic fields.^{6,9-11}

In the presence of strong localization and in the regime of the variable-range hopping the negative magnetoresistance associated with the quantum interference effects was observed in highly disordered In₂O_{3-x} films^{5,12} and in compensated GaAs.¹³ The publications relevant to the experimental

study of weak localization in doped semiconductors can also be found in Refs. 14 and 15. It is clear that quantum interference depends on both electron density and disorder. However, in doped semiconductors, where disorder is produced by a random impurity potential, a variation of disorder is always accompanied by a corresponding variation of the electron concentration. Therefore, in this case a careful analysis of the temperature and magnetic-field dependencies of the conductivity are indispensable in order to separate the effects of the interaction and disorder on the quantum interference.^{16,17} On the other hand, semiconductor superlattices present an electron system where disorder can be controlled independently of the electron concentration. In the so-called intentionally disordered superlattices firstly considered in Ref. 18, disorder is introduced during the growth by a random variation of the periodicity. At not very high doping concentrations this artificial disorder can dominate the disorder due to impurities. In this case the disorder strength can be completely controlled by a superlattice structure, while impurities supply the carriers. In such electron systems the weak localization can be studied in a wide range of disorder strengths—from almost perfectly ordered superlattices, where the transport is due to the extended electron states, to structures where the strong disorder induces spatially localized electron levels. The first observation of the electron localization in the intentionally disordered GaAs/Al_xGa_{1-x}As superlattices was presented in Ref. 19.

Weak-localization corrections to the conductivity of the disordered semiconductor superlattices were recently considered in Ref. 20 in two limits: a strong disorder along the growth direction z , when $t_z \tau < \hbar$ (where t_z is the coupling energy along z and τ is the elastic scattering time), and a weak scattering with $t_z \tau > \hbar$. In both cases a weak in-plane disorder ($E_F \tau \gg \hbar$) was supposed. In the first case an electron experiences many scatterings before leaving a layer.

This is the diffusive Fermi-surface (DFS) regime, opposite to the second case of the weak scattering regime characterized by the usual propagative Fermi surface (PFS). It was shown that the strong vertical disorder modifies the parallel transport resulting in a very different shape of the magnetoconductivity caused by the quantum corrections than that one corresponding to the PFS regime.

In the regime of the propagative Fermi surface the weak localization effects were studied in the GaAs/Al_xGa_{1-x}As superlattices in Refs. 21 and 22, while the anisotropy of the negative magnetoresistance was investigated in relatively high doped GaAs/Al_xGa_{1-x}As superlattices in a regime close to the DFS one in Ref. 23.

Intentionally disordered superlattices, where disorder is introduced by a controlled random variation of well thicknesses, are excellent candidates to model the electron system considered in Ref. 20 and thus, to study the effects of the vertical disorder on the parallel transport. In such superlattices the disorder reveals the anisotropic character when the electrons can be localized along the growth direction, while moving freely in the plane of the wells.

In this paper we explore the weak localization in intentionally disordered short-period doped GaAs/Al_xGa_{1-x}As superlattices in wide ranges of the disorder strengths and doping levels. In all the samples we found the characteristic features of the DFS regime with a tendency toward the PFS one observed with the increase of the electron density.

The paper is organized as follows. The theory is considered in Sec. II. The electronic properties of the samples are characterized in Sec. III. The experimental results and discussion are given in Sec. IV, while conclusions are outlined in Sec. V.

II. THEORY

Following Ref. 20, we will consider the transport properties of a superlattice in a weak-field regime ($\omega_c \tau \ll 1$). The vertical motion (parallel to the growth direction) is coherent when the elastic time $\tau \gg \hbar/t_z$. On the other hand, the coherent motion breaks down when $\tau \ll \hbar/t_z$, which corresponds to a localization of an electron on a length scale smaller than the period of a superlattice. In the first case the electrons propagatively move in a coherent band, and the use of a quasiclassical formalism is justified. However, in the second case the electron transport may occur as a hopping process between the neighboring wells, which is a diffusive process. In the later case the broadening of the Fermi surface along the z direction is larger than the width of the energy dispersion t_z . Consequently, one distinguishes two regimes: the regime of the propagative Fermi surface and the regime when the Fermi surface becomes diffusive—the DFS one. In the regime of a PFS a formula for the quantum correction to the classical conductivity was obtained,²⁴

$$\delta\sigma_{\parallel}(H) - \delta\sigma_{\parallel}(0) = \frac{e^2}{2\pi^2\hbar l_H} \alpha F(\delta), \quad (1)$$

where $l_H = \sqrt{\hbar/eH}$ is the magnetic length, $\alpha = \sqrt{D_{\parallel}/D_z}$ is the coefficient of the anisotropy, D_{\parallel} and D_z are the diffu-

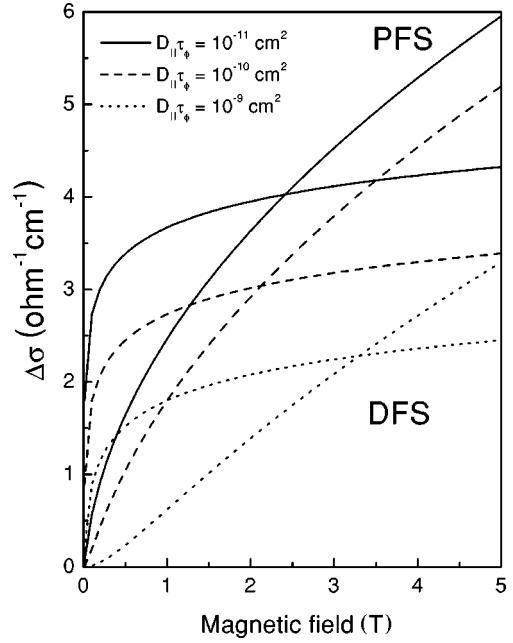


FIG. 1. Quantum corrections to the classical conductivity calculated in two transport regimes (PFS and DFS) according to Eqs. (1) and (2), with different values $D_{\parallel}\tau_{\varphi}$.

sion coefficients parallel and perpendicular to the layers respectively, $F(\delta) = \sum_{n=0}^{\infty} 2[(n+1+\delta)^{1/2} - (n+\delta)^{1/2}] - (n+\frac{1}{2}+\delta)^{-1/2}$ is the Kawabata function²⁵ with $\delta = l_H^2/4D_{\parallel}\tau_{\varphi}$, and τ_{φ} is the electron wave-function dephasing time.

In the case of a strongly DFS another formula was obtained,²⁰

$$\delta\sigma_{\parallel}(H) - \delta\sigma_{\parallel}(0) = -\frac{e^2}{2\pi^2\hbar d_{SL}} F(\delta, \delta'), \quad (2)$$

where d_{SL} is the period of a superlattice,

$$F(\delta, \delta') = \sum_{n=0}^{\infty} \frac{1}{\sqrt{n+\frac{1}{2}+\delta} \sqrt{n+\frac{1}{2}+\delta'}} - 2 \ln(\sqrt{n+1+\delta} + \sqrt{n+1+\delta'}) + 2 \ln(\sqrt{n+\delta} + \sqrt{n+\delta'}),$$

with

$$\delta' = \frac{l_H^2}{4D_{\parallel}} \left(\frac{1}{\tau_{\varphi}} + 2 \frac{t_z^2 \tau}{\hbar^2} \right).$$

The essential difference between Eqs. (1) and (2) is in the prefactors multiplying the functions $F(\delta)$ and $F(\delta, \delta')$. It includes the magnetic length l_H or the superlattice period d_{SL} in the PFS or DFS regimes, respectively. This produces very different shapes of the weak-localization magnetoresistance in both regimes, as shown in Fig. 1, where the weak-localization corrections were calculated with different pa-

rameters $D_{\parallel}\tau_{\phi}$ entering Eqs. (1) and (2). Contrary to the PFS regime, the magnetoresistance calculated in the DFS regime reveals a much stronger dependence at very weak magnetic fields with a tendency to saturate with the increase of the magnetic field.

In the presence of vertical localization the coupling energy t_z is replaced by the tunneling rate. Estimates show that in this case $1/\tau_{\phi} \gg 2(t_z^2\tau/\hbar^2)$, and therefore a good approximation is $\delta' \approx \delta$.

III. CHARACTERIZATION OF THE SAMPLES

In order to control the disorder strength, the $(\text{GaAs})_m(\text{Al}_{0.3}\text{Ga}_{0.6}\text{As})_6:\text{Si}$ superlattices were prepared with a fixed doping. The vertical disorder was produced by a controlled random variation of the GaAs well thicknesses around the nominal value $m=17$ ML, corresponding to a Gaussian distribution of the lowest levels of noninteracting electrons forming the conduction miniband. The barrier thicknesses were unchanged.

According to the calculations made by the Kronig-Penney model including the potential nonparabolicity, the width of the lowest Γ miniband of the nominal superlattice $(\text{GaAs})_{17}(\text{Al}_{0.3}\text{Ga}_{0.6}\text{As})_6$ is $W=55$ meV. The doping concentrations were chosen in order to obtain the samples with a partial occupation of the miniband ($E_F=32$ meV at $N=6.0 \times 10^{17} \text{ cm}^{-3}$) and with a completely full miniband ($E_F=52$ meV at $N=1.7 \times 10^{17} \text{ cm}^{-3}$). The samples were grown by molecular beam epitaxy on (100)-oriented GaAs substrates. In order to avoid the short-range in-plane fluctuations, the growth of the superlattices was interrupted for 20 sec at the normal interface and for 3–5 sec at the inverted one. The total number of 50 periods was grown. The disorder strength was uniquely characterized by the disorder parameter $\delta=\Delta/W$, where Δ is the full width at half maximum of a Gaussian distribution of the electron energy calculated in the isolated quantum well, and W is the miniband width of the nominal superlattice in the absence of disorder. Even in the nominal superlattices the unavoidable monolayer fluctuations produce the vertical disorder strength $\delta \approx 0.18$. One expects that at $\delta \approx 1$ majority of the electrons moving in the miniband perpendicular to the layers should be localized. The localization of the vertically moving electrons was detected in the studied here superlattices by Raman scattering in Ref. 26.

The samples were patterned into Hall bars prepared by standard lithography and chemical etching. The Ohmic contacts were fabricated by depositing an Au-Ge-Ni alloy. A conventional ac four-probe method was used to measure resistivity. The values of the Hall in-plane mobilities measured at $T=4.2$ K were found in the interval from 600 to 1500 cm^2/Vs , which results in the values $k_F\lambda \approx 3-9$. This implies a quasi-metallic character of the in-plane conductivity, as supposed in Ref. 20. The parallel magnetoresistance measurements were performed in the ‘‘Oxford Instruments’’ superconducting magnet system at $T=1.7$ K. The magnetic field was directed along the growth direction (z) of the superlattices.

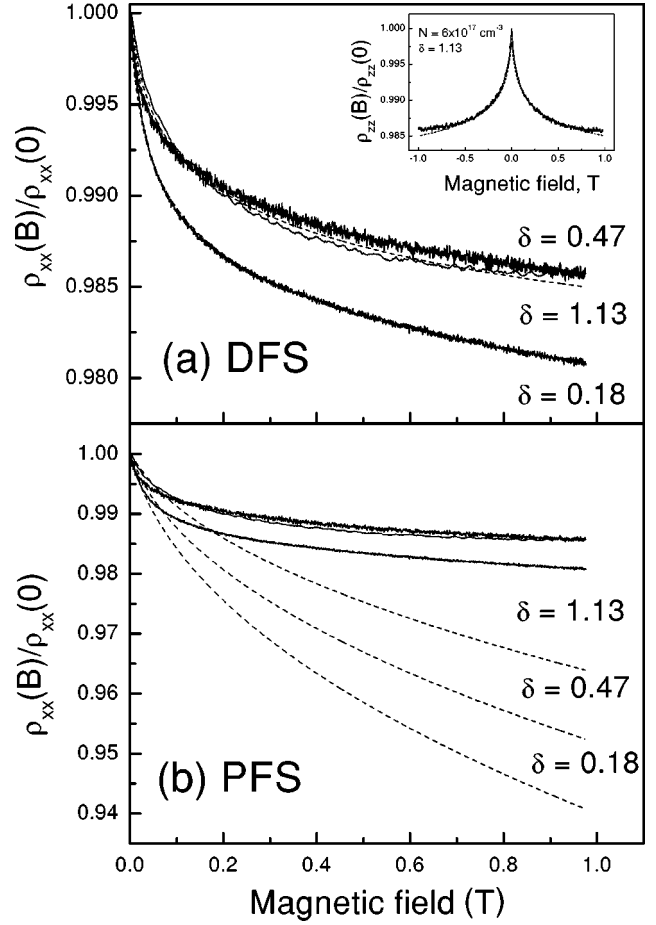


FIG. 2. Magnetoresistances measured in the disordered GaAs/Al_xGa_{1-x}As superlattices with a fixed doping concentration $N=6.0 \times 10^{17} \text{ cm}^{-3}$ and different disorder strengths. A comparison is shown with the magnetoresistance calculated in a DFS (a) and in a PFS (b) transport regimes (dashed lines). The inset shows the magnetoresistance measured in the magnetic fields of the opposite orientations.

IV. RESULTS AND DISCUSSION

The magnetoresistances measured in the intentionally disordered GaAs/Al_xGa_{1-x}As superlattices with different doping concentrations and disorder strengths are shown for some of the samples in Figs. 2 and 3. The observed symmetry of the low-field negative magnetoresistance caused by the quantum interference, shown in the insertion in Fig. 2(a) for one of the superlattices with the highest disorder strength, gives a proof of the macroscopic in-plane homogeneity of the samples.²⁷

In all the here studied superlattices we found the best agreement with the magnetoresistance calculated in a DFS regime [Eq. (1)] than in a PFS one [Eq. (2)]. The dependences calculated for a PFS regime shown in Fig. 2(b) were fitted in the low-field range and then extrapolated to the high magnetic fields. As it was mentioned in Sec. II, the observed difference in the magnetoresistance mainly comes from the prefactor of Eqs. (1) and (2). In the PFS regime it depends on the magnetic field through the magnetic length l_H , while in the case of strong disorder the magnetic length is substituted

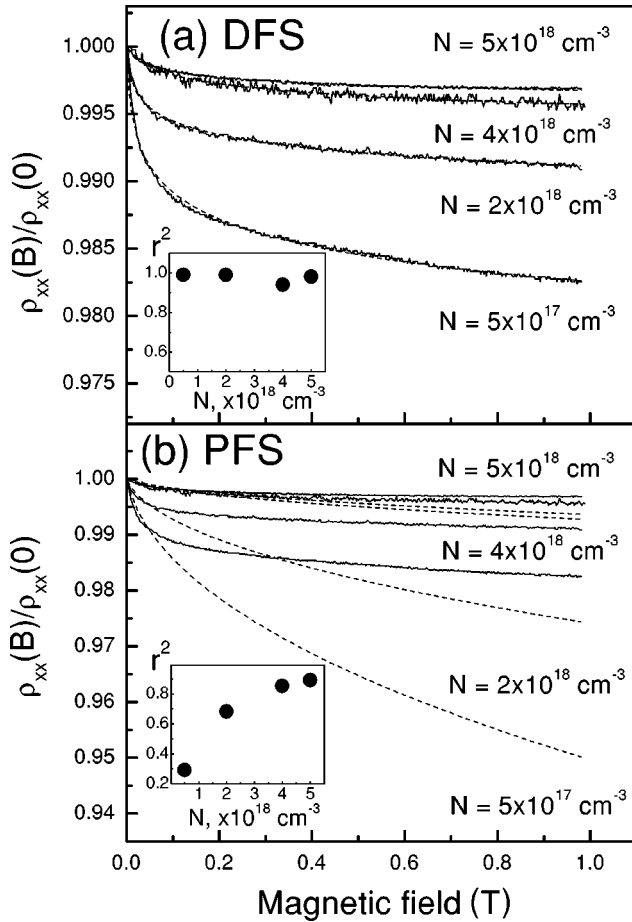


FIG. 3. Magnetoresistances measured in the disordered $\text{GaAs}/\text{Al}_x\text{Ga}_{1-x}\text{As}$ superlattices with a fixed disorder strength $\delta = 0.18$ and different doping concentrations. A comparison is shown with the magnetoresistance calculated in DFS (a) and PFS (b) transport regimes (dashed lines). The insets show the concentration dependence of the coefficient of determination thus far achieved during the least-squares fitting (r^2).

by the superlattice period d_{SL} . Therefore, the magnetoresistance of the strongly disordered superlattices is completely associated with the function $F(\delta, \delta')$.

It is clear that the effect of disorder on the magnetoresistance should decrease with increasing electron density. This is because with the increase of the electron concentration, when $E_F > \Delta$, the condition $\hbar/\tau > t_z$ changes to $\hbar/\tau < t_z$. Therefore, we expect that an increase of the electron concentration should result in a transition from a DFS regime to a PFS one. As a consequence, the magnetoresistance measured in the highly doped disordered superlattices, instead following the magnetoresistance calculated with Eq. (2), should approximate the value calculated according to Eq. (1). Indeed, as is shown in Fig. 3(b), the better fitting of the calculated according to the PFS formula magnetoresistance can be obtained with increasing electron concentration, while no improvement of the fitting made by the PFS formula was obtained with the variation of the disorder strength [Fig. 2(b)]. The inset to Fig. 3(b) exhibits the values of the coefficient of determination thus far achieved during the least-squares fitting (r^2), which significantly increases with the

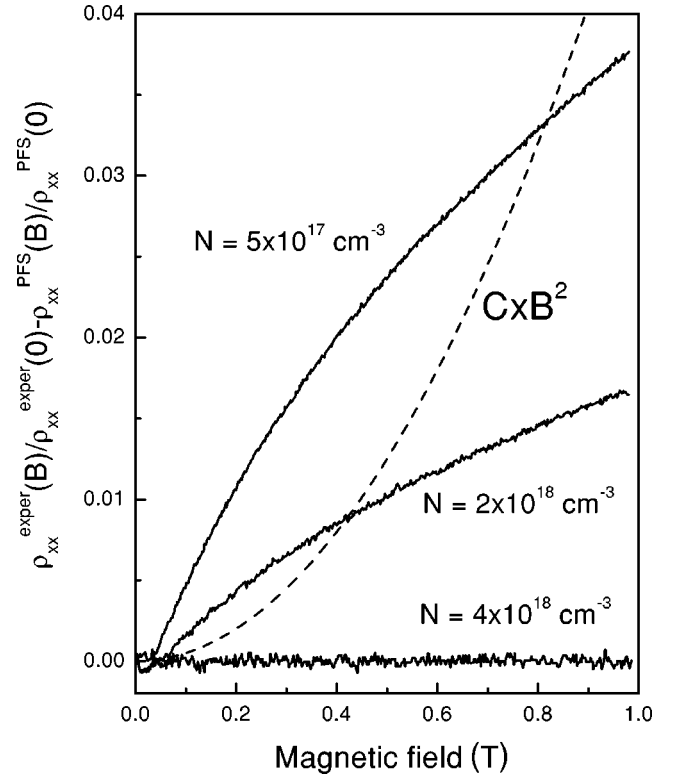


FIG. 4. Differences between the magnetoresistances measured in the differently doped superlattices $(\text{GaAs})_{17}(\text{Al}_{0.3}\text{Ga}_{0.7}\text{As})_6$ with $\delta = 0.18$ and the magnetoresistances calculated in a PFS regime. The dashed line shows the quadratic field dependence (C is the constant).

concentration showing the improvement of the fitting. Conversely, good fittings obtained with the DFS formula for all the samples independently of the concentration are demonstrated in the inset to Fig. 3(a). A better suitability of Eq. (1) in highly doped superlattices is also presented in Fig. 4, where the differences between the measured magnetoresistances and the magnetoresistances calculated according to the PFS formula revealed clear decrease with increasing concentration.

The ratios of the relative resistivities calculated in a PFS regime at $B = 1$ T to the lateral resistivities measured at the same magnetic field ($\rho_{PFS}/\rho_{\text{expt}}$) presented in Fig. 5 again show a better accordance between them obtained with the increase of the electron concentration [Fig. 5(a)]. While, an opposite behavior of the ratios $\rho_{PFS}/\rho_{\text{expt}}$ revealed the slight enhancement of the disagreement between the PFS formula and the experimental data with increasing disorder [Fig. 5(b)].

It is worth mentioning that the differences between the measured magnetoresistances and that ones calculated according to the formula for a PFS regime [Eq. (2)], which are plotted in Fig. 4, do not reveal a quadratic dependence and therefore, cannot be assigned to the contribution of the positive classical magnetoresistance. Thus we concluded that the DFS transport regime was undoubtedly found in all the low-doped disordered superlattices under investigation with no signatures of the PFS regime. In highly doped superlattices

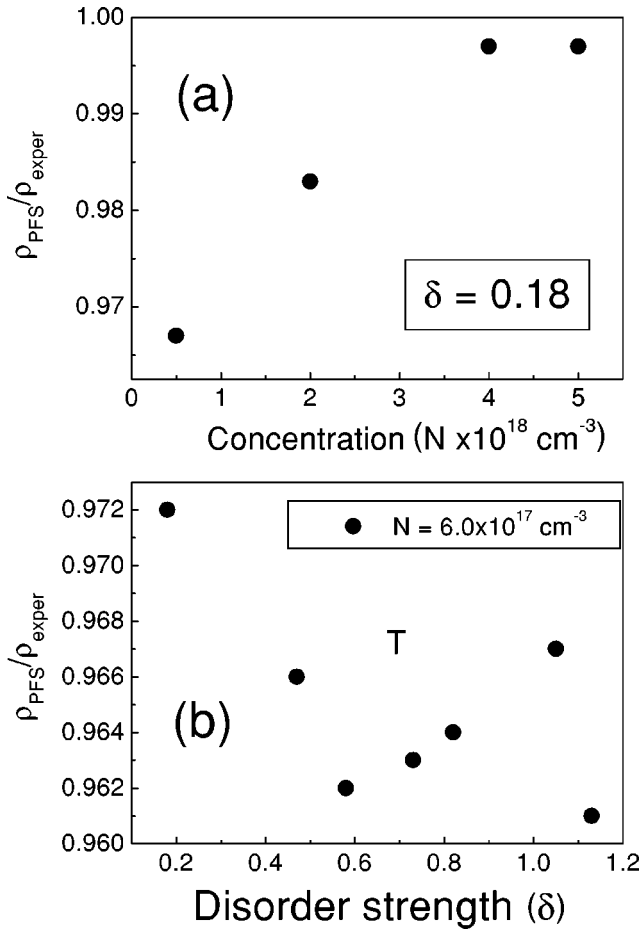


FIG. 5. Ratios of the relative resistivities calculated in a PFS regime at $B=1$ T (ρ_{PFS}) to the relative resistivities measured at the same magnetic field (ρ_{exper}), obtained in the superlattices with a fixed disorder ($\delta=0.18$) and different doping concentrations (a) and with fixed doping concentration ($N=6.0 \times 10^{17} \text{ cm}^{-3}$) and various disorder strengths (b).

with relatively weak disorder, a tendency to the PFS regime was observed.

It also ought to be stressed that calculations of the quantum correction to the classical conductivity in the hopping conductivity regime, mentioned in Sec. I, yield a quadratic dependence for small magnetic fields, which does not account for the negative magnetoresistance observed here. Probably, this is caused by different characters of conductivities: the variable-range hopping transport considered in Refs. 6, 8, and 11 and the quasimetallic in-plane conductivity found in the studied here disordered doped superlattices.

The fitting of the magnetoresistance calculated in the DFS regime [Eq. (2) with $\delta' \approx \delta$, as explained in the end of Sec. II] to the experimental curves allowed us to obtain the decoherence time (τ_φ). The weak-localization parameters $D_{\parallel}\tau_\varphi$ corresponding to the best fitting were used to extract τ_φ when the diffusion coefficient D_{\parallel} was determined by the measurements of the resistivity ρ_{xx} according to the Einstein relation for the degenerate electron gas. The values of the decoherence time measured as a function of the disorder strength and the doping concentration are shown in Figs. 6(a)

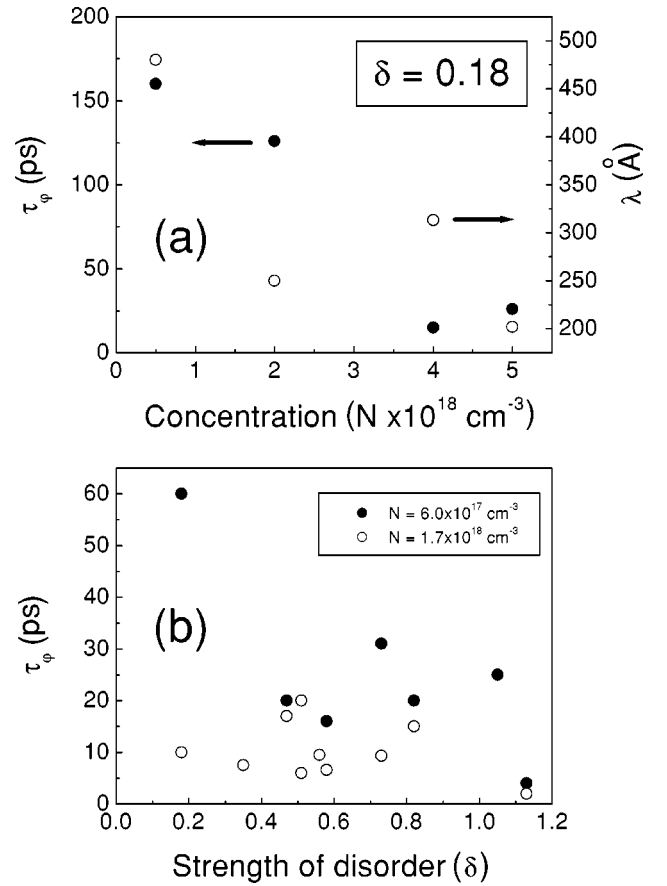


FIG. 6. Dephasing times obtained by the fitting of the magnetoresistance calculated in the DFS regime to the experimental magnetoresistances measured in the superlattices with a fixed disorder ($\delta=0.18$) and different doping concentrations: (a) and with fixed doping concentrations ($N=6.0 \times 10^{17}$ and $1.7 \times 10^{18} \text{ cm}^{-3}$) and various disorder strengths (b). Open circles in (a) show the values of the electron mean free paths (λ) obtained by means of the conductivity measurements.

and 6(b). It is worth mentioning, that according to Ref. 28 expressions (1) and (2) obtained in the diffusion approximation overestimate the value of the weak-localization correction and therefore, the true values of the dephasing times is expected to be somewhat smaller than those obtained by the fitting. However, the qualitative behavior of the dephasing time will not change by this systematic error.

Usually, two contributions to the electron wave-function dephasing are considered: one due to the electron-electron interaction (τ_{ee}) and another one due to the electron-phonon interaction (τ_{ph}).^{14,15} However, as is known, at low temperatures the electron-electron interaction produces the dominant contribution to the electron wave-function dephasing in the superlattices (see Ref. 29, and references therein). In accordance with Ref. 30, the rate of the electron-electron collisions depends on the value of momentum transfer. In the case of small momentum transfer $k \ll k_s$ (where k_s is the inverse screening length),

$$\tau_{ee,S} = \left(\frac{k_B T}{k_F \lambda} \right)^{3/2} \frac{\sqrt{3}}{4 \sqrt{E_F}}, \quad (3)$$

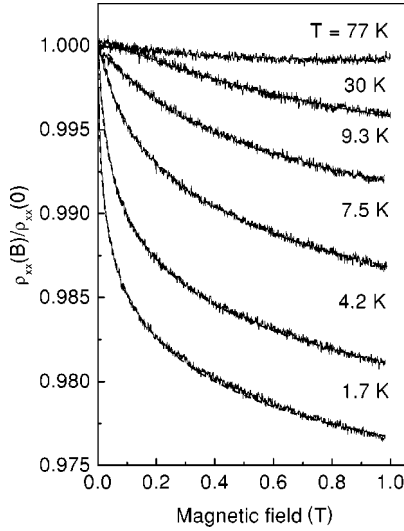


FIG. 7. Relative magnetoresistances measured at various temperatures in the superlattices $(\text{GaAs})_{17}(\text{Al}_{0.3}\text{Ga}_{0.7}\text{As})_6$ with the electron concentration $N=6.0 \times 10^{17} \text{ cm}^{-3}$ and the disorder strength $\delta=0.18$. The dashed lines were calculated in the DFS regime.

while processes with a large momentum transfer yield a scattering rate

$$\frac{\hbar}{\tau_{ee,L}} = \frac{(k_B T)^2 k_s}{\hbar E_F k_F}. \quad (4)$$

As follows from these expressions, the increase of the electron density should result in an increase of the dephasing time. Conversely, our experimental data presented in Fig. 6(a) exhibit the decrease of the dephasing time with an increase of the doping concentration. The observed decrease of the dephasing time can be associated with the dominant decrease of the mean free path in Eq. (4) with doping. The values of the electron mean free paths obtained by means of the parallel conductivity measurements, which are shown in Fig. 6(a) by open circles, indeed reveal a decrease with the increase of the doping. This shows that in weakly disordered superlattices collisions with small momentum transfers dominate. The same processes with the small momentum transfer probably govern the dependence of the dephasing time with the disorder strength found in the low-doped superlattices [closed circles in Fig. 6(b)], where the electron density is fixed while the mean free path decreases with increasing disorder. With an increase of the electron density the screening effects become stronger, resulting in a limitation of the momentum transfers. Therefore, the collisions with a large momentum transfer mainly contribute to the electron-electron scattering rate in the highly doped disordered superlattices where, according to Eq. (4), the dephasing time depends only on the electron concentration and the temperature which were fixed; therefore, $\tau_{ee,L}$ should not be influenced by disorder.

The temperature dependence of the magnetoresistance measured in the studied superlattices is shown in Fig. 7. An excellent accordance between the experimental data and the

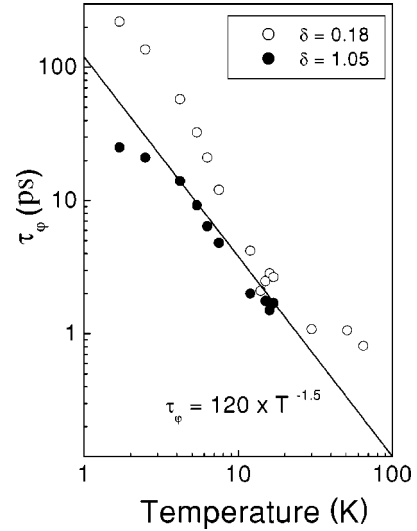


FIG. 8. Temperature dependencies of the dephasing time τ_ϕ measured in the disordered superlattices $(\text{GaAs})_m(\text{Al}_{0.3}\text{Ga}_{0.7}\text{As})_6$ with the electron concentration $6.0 \times 10^{17} \text{ cm}^{-3}$ and with different disorder strengths $\delta=0.18$ (open circles) and $\delta=1.05$ (closed circles).

magnetoresistance calculated in the DFS regime [Eq. (2)] was found up to rather high temperatures. The values of the dephasing time τ_ϕ obtained at different temperatures by the fitting of the calculated magnetoresistance to the measured one are plotted in Fig. 8. At such temperatures the electron-electron interaction is expected to dominate in the dephasing process, yielding power dependencies (4) and (5) of the dephasing time on the temperature predicted theoretically in Ref. 30. In the relevant temperature range (between 1 and 10 K) the dependence corresponding to the small momentum transfers [Eq. (4)] was found in the regular $\text{GaAs}/\text{Al}_x\text{Ga}_{1-x}\text{As}$ superlattices in Ref. 29. Our data do not clearly reveal such a power dependence; this implies that the dephasing processes in the presence of the strong localization and without it are probably different. The dependence of the dephasing time corresponding to Eq. (4) is shown in Fig. 8 as a reference.

We would like to point out that the effects of the diffusive Fermi surface observed here can influence the quantum interference even in the nominally regular superlattices where either the monolayer fluctuations or the interface roughnesses may provide the disorder. It is not clear whether or not such effects could be found in the superlattices studied in Ref. 29, where the measurements were presented in very weak magnetic fields. An indication of the discrepancy between the experiment and the theory can be found in Ref. 23, where the magnetoresistance of the short-period superlattices was studied in the magnetic fields up to 1 T.

Finally, we would like to discuss briefly a problem of the electron-electron interaction. An exhaustive analysis of the contributions from the interaction corrections to the conductivity of the superlattices was performed in Ref. 29. It was demonstrated that the electron-electron interaction effects cannot account for the negative magnetoresistance in superlattices at magnetic fields much lower than the elastic field

$B_e = \hbar/4eD_{\parallel}\tau_e$, which in our case of the low-mobility samples is estimated to be equal to 7–12 T. A relatively small positive magnetoresistance superimposed on a large negative magnetoresistance can stem from the spin effects at fields much higher than $B_s = kT/g^*\mu_B$, which is around 0.1 T in our case, while the orbital effects result in an insignificant contribution at low temperatures. Therefore, in the here studied superlattices we do not expect an appreciable influence of the electron-electron interaction effects to the measured negative magnetoresistance.

V. CONCLUSIONS

The processes of weak localization were studied in the intentionally disordered doped short-period GaAs/Al_xGa_{1-x}As superlattices where the disorder strength and the electron density can be controlled independently. Two different transport regimes were considered: the regime of weak disorder characterized by the propagative Fermi surface and the regime of strong disorder with the corresponding diffusive Fermi surface. For the low-doped disordered superlattices we found the diffusive transport regime, while a tendency to the propagative regime was observed with the

increase of the electron concentration. This result manifests to itself in the influence of the vertical disorder on the quantum corrections to the in-plane conductivity of the semiconductor superlattices predicted in Ref. 20.

The decrease of the dephasing of the electron wavefunction was observed with the increase of both the doping concentration and the disorder strength, which suggests the importance of the electron-electron collisions with small momentum transfer. We did not find any significant influence of disorder on the dephasing process in the heavily doped superlattices, where the Fermi energy exceeded the random potential fluctuations. The temperature dependence of the dephasing time implies that the dephasing process observed in disordered GaAs/Al_xGa_{1-x}As superlattices is different from that found in regular superlattices.

ACKNOWLEDGMENTS

We are indebted to Professor M.S. Li for the help in the realization of the temperature-dependent measurements, and to H. Arakaki and C.A. de Souza for technical assistance. Financial support from FAPESP is gratefully acknowledged.

-
- ¹E. Abrahams, P.W. Anderson, D.C. Licciardello, and T.V. Ramakrishnan, Phys. Rev. Lett. **42**, 673 (1979).
²B.L. Al'tshuler and A.G. Aronov, Zh. Éksp. Teor. Fiz. **77**, 2028 (1979) [Sov. Phys. JETP **50**, 968 (1979)].
³B.L. Al'tshuler and A.G. Aronov, in *Electron-electron Interaction in Disordered Conductors*, edited by A.L. Efros and M. Pollak (North-Holland, Amsterdam, 1985).
⁴P.A. Lee and T.V. Ramakrishnan, Rev. Mod. Phys. **57**, 287 (1985).
⁵O. Farah and Z. Ovadyahu, Phys. Rev. B **38**, 5457 (1988).
⁶P. Kleinert and V.V. Bryksin, Phys. Rev. B **55**, 1469 (1997).
⁷V.I. Nguyen, B.Z. Spivak, and B.I. Shklovskii, Pis'ma Zh. Éksp. Teor. Fiz. **41**, 35 (1985) [JETP Lett. **41**, 42 (1985)].
⁸U. Sivan, O. Entin-Wohlman, and Y. Imry, Phys. Rev. Lett. **60**, 1566 (1988).
⁹D. Vollhardt and P. Wölfle, Phys. Rev. B **22**, 4666 (1980).
¹⁰V.V. Bryksin and P. Kleinert, Z. Phys. B: Condens. Matter **101**, 91 (1996).
¹¹O. Bleibaum, H. Böttger, and V.V. Bryksin, Phys. Rev. B **64**, 104204 (2001).
¹²Z. Ovadyahu, Phys. Rev. B **33**, 6552 (1986).
¹³M. Benzaquen, D. Walsh, and K. Mazuruk, Phys. Rev. B **38**, 10 933 (1988).
¹⁴G. Bergmann, Phys. Rep. **107**, 1 (1984).
¹⁵T.A. Polyanskaya and Yu. V. Shmartsev, Fiz. Tekh. Poluprovodn. **23**, 3 (1989) [Sov. Phys. Semicond. **23**, 1 (1989)].
¹⁶G.M. Minkov, O.E. Rut, A.V. Germanenko, A.A. Sherstobitov, V.I. Shashkin, O.I. Krohin, and V.M. Daniltsev, Phys. Rev. B **64**, 235327 (2001).
¹⁷P.T. Coleridge, A.S. Sachrajda, and P. Zawadzki, Phys. Rev. B **65**, 125328 (2001).
¹⁸J.D. Dow, S.Y. Ren, and K. Hess, Phys. Rev. B **25**, 6218 (1986).
¹⁹A. Chomette, B. Deveaud, A. Regreny, and G. Bastard, Phys. Rev. Lett. **57**, 1464 (1986).
²⁰A. Cassam-Chenai and D. Mailly, Phys. Rev. B **52**, 1984 (1995).
²¹W. Szott, C. Jedrzejek, and W.P. Kirk, Phys. Rev. Lett. **63**, 1980 (1989).
²²A.B. Gougam, J. Sicart, and J.L. Robert, J. Phys. III (France) **7**, 133 (1997).
²³A.B. Gougam, J. Sicart, J.L. Robert, and B. Etienne, Phys. Rev. B **59**, 15 308 (1999).
²⁴W. Szott, C. Jedrzejek, and W.P. Kirk, Phys. Rev. B **40**, 1790 (1989).
²⁵A. Kawabata, J. Phys. Soc. Jpn. **49**, 628 (1980).
²⁶Yu.A. Pusep, W. Fortunato, P.P. Gonzalez-Borrero, A.I. Toropov, and J.C. Galzerani, Phys. Rev. B **63**, 115311 (2001).
²⁷W. Szott, E. Palm, and W.P. Kirk, Bull. Am. Phys. Soc. **33**, 821 (1988).
²⁸G.M. Minkov, A.V. Germanenko, V.A. Larionova, S.A. Negashev, and I.V. Gornyi, Phys. Rev. B **61**, 13 164 (2000).
²⁹W. Szott, C. Jedrzejek, and W.P. Kirk, Phys. Rev. B **48**, 8963 (1993).
³⁰B.L. Al'tshuler and A.G. Aronov, Pis'ma Zh. Éksp. Teor. Fiz. **30**, 514 (1979) [JETP Lett. **30**, 482 (1979)].